Cell Stem Cell, Volume *20*

Supplemental Information

Predictive Markers Guide Differentiation to Improve Graft Outcome in Clinical Translation of hESC-Based Therapy for Parkinson's Disease

Agnete Kirkeby, Sara Nolbrant, Katarina Tiklova, Andreas Heuer, Nigel Kee, Tiago Cardoso, Daniella Rylander Ottosson, Mariah J. Lelos, Pedro Rifes, Stephen B. Dunnett, Shane Grealish, Thomas Perlmann, and Malin Parmar

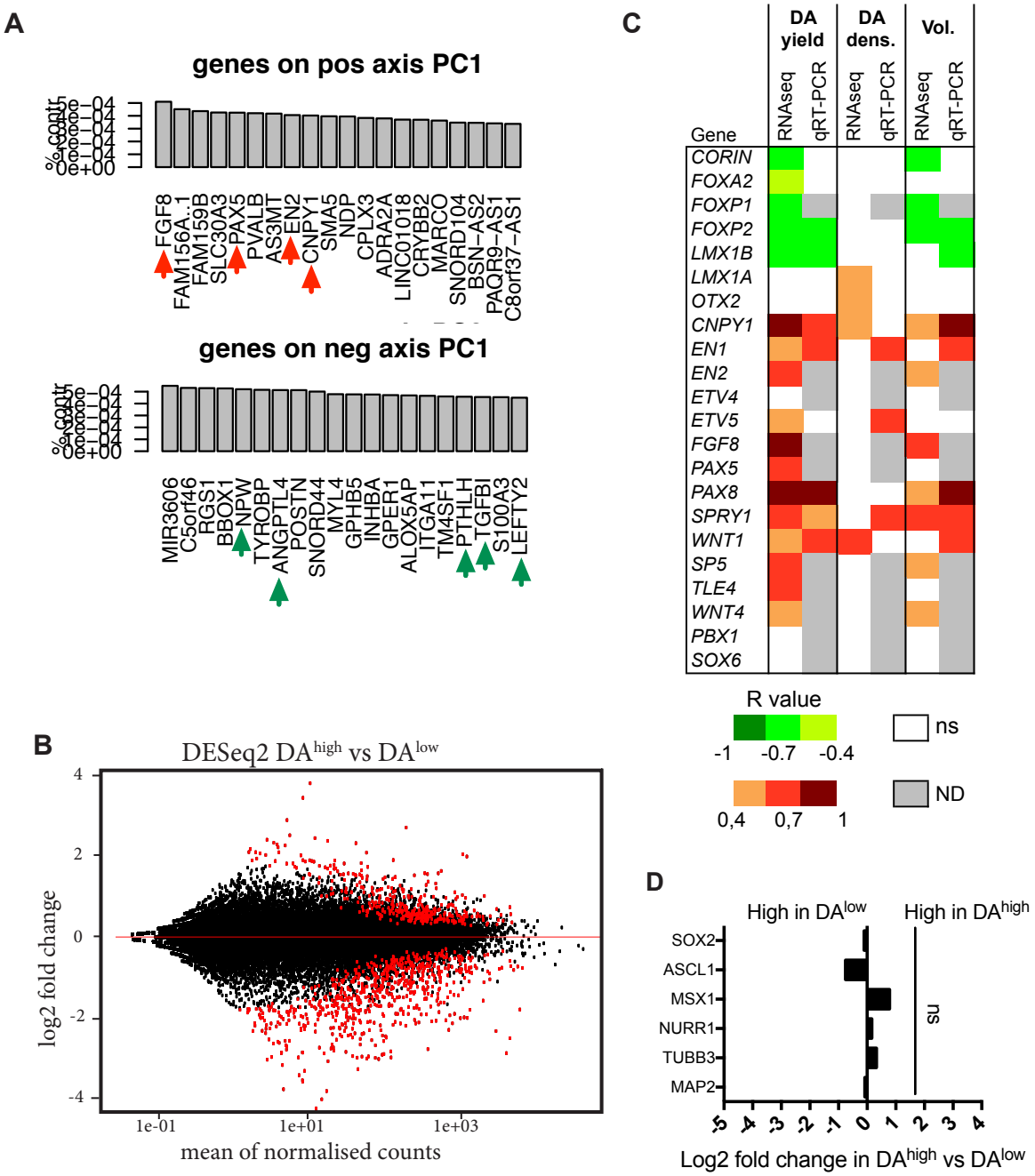

Figure S1. Gene expression correlations to graft outcome (related to Figure 2). (**A**) Results from main gene cluster at positive and negative PCA axis PC1 (from Figure 2B). Genes related to expression in the MHB domain are marked by red arrows and genes related to expression in diencephalic domains are marked with green arrows. (**B**) DESeq2 plot showing all differentially expressed genes as red dots (only genes with an adjusted $p<0.01$). (**C**) Overview of positive and negative correlations between gene expression levels to the 3 parameters of graft outcome: DA yield (TH+ cells per 100,000 cells grafted), DA density (TH+ cells per mm^3) and volume (Vol: mm^3 per 100,000 cells grafted) using samples from the DA-high and DA-low groups based on either qRT-PCR analysis or RNAseq RPKM values. Correlations are color coded according to the Spearman correlation R values only for correlations with $p<0.05$. White shading denotes non-significant (ns) correlations and grey shading is applied for genes that have not been assessed by qRT-PCR (ND: not determined). (**D**) Markers of proliferative DA progenitors (*SOX2*, *ASCL1* and *MSX1*) and markers of postmitotic DA progenitors (*NURR1*, *TUBB3* and *MAP2*) were found to not be differentially expressed in the DA-high versus DA-low group in the DESeq2 analysis (ns = non-significant)

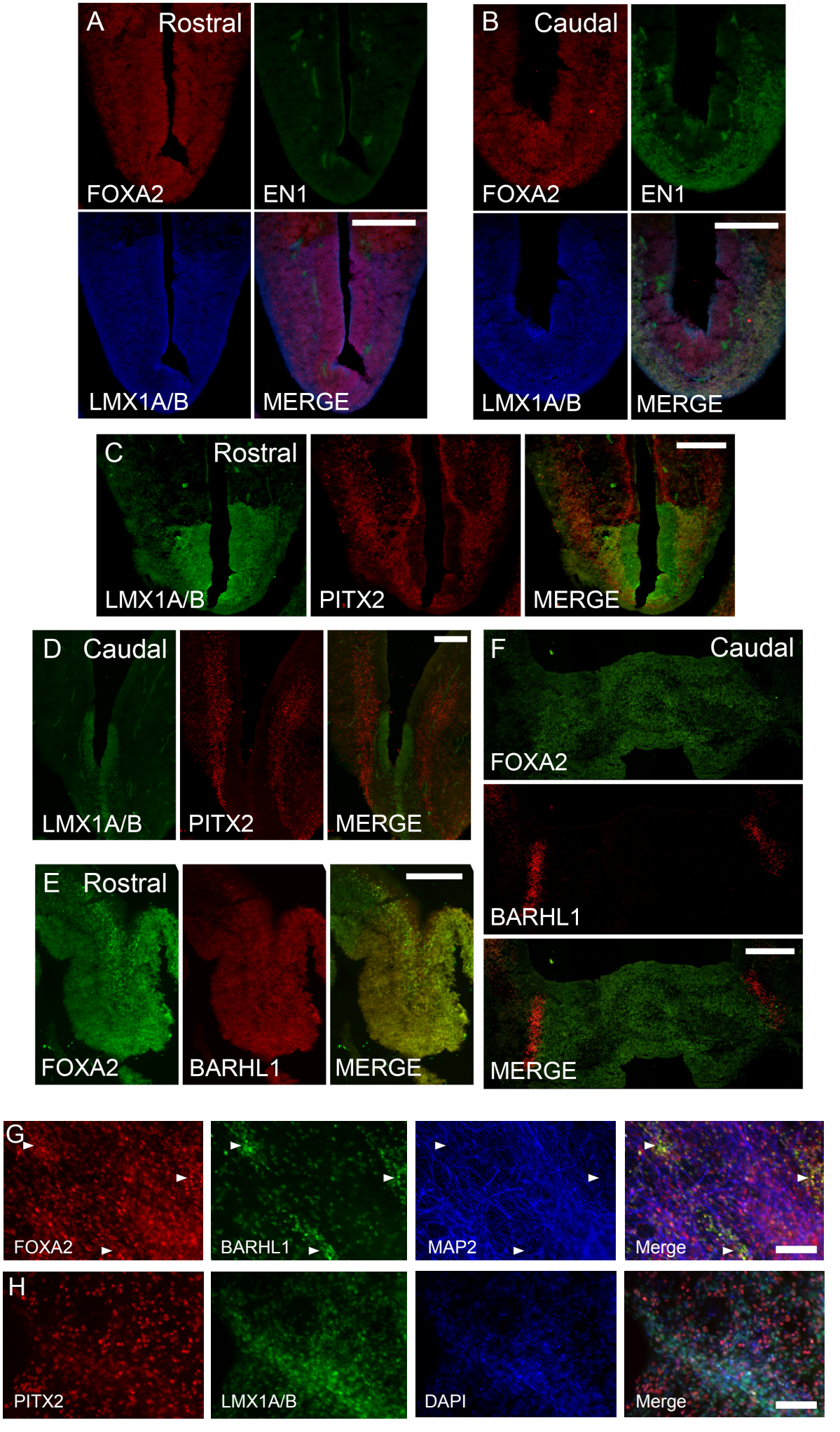
A Rostral
FOXA2
EN1
LMX1A/B
MERGE
B Caudal
FOXA2
EN1
LMX1A/B
MERGE
C Rostral
LMX1A/B
PITX2
MERGE
D Caudal
LMX1A/B
PITX2
MERGE
E Rostral
FOXA2
BARHL1
MERGE
F Caudal
FOXA2
BARHL1
MERGE
G
FOXA2
BARHL1
MAP2
Merge
H
PITX2
LMX1A/B
DAPI
Merge

Figure S2. Human fetal tissue expression patterns and terminal *in vitro* differentiation of cultures with STN fates (related to Figure 3)

(**A-F**) Immunostainings of human fetal brain tissue shows differential staining for PITX2, BARHL1 and EN1 within the FOXA2+/LMX1A/B+ rostral and caudal domains as visualised schematically in Fig 3D. Sections were sampled from embryos of the following gestational time points: A, B, C, E: 6.5 wk p.c. D: 9.5 wk p.c. F: 7.5 wk p.c. (**G+H**) Terminal neuronal differentiation of VM-patterned cultures (d42) show persistent presence of G) FOXA2+/BARHL1+ and H) PITX2+/LMX1A+ cells. Scale bars: A, B, C, D, E: 200 μm. F: 500 μm. G, H: 100 μm

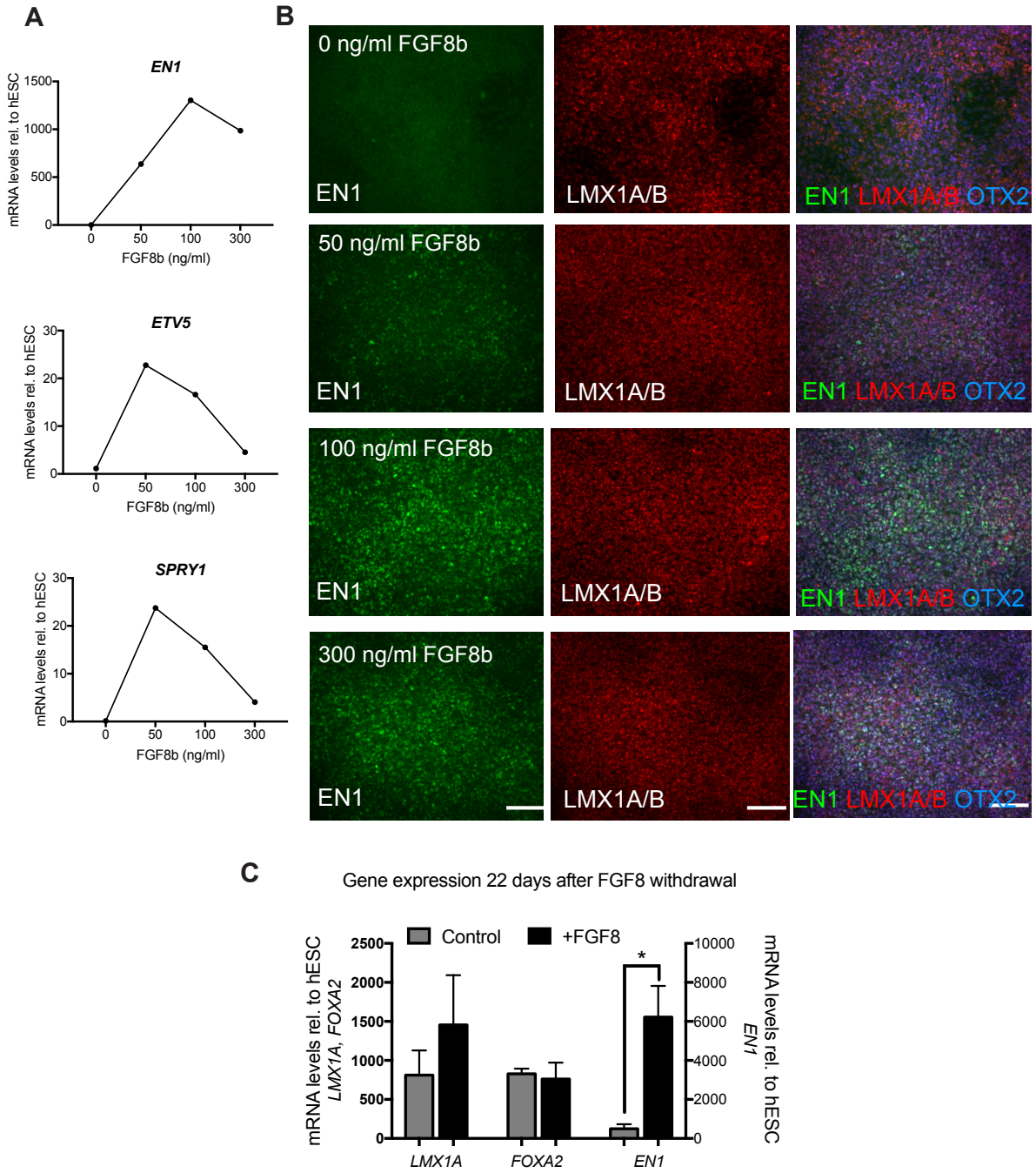

Figure S3. Optimisation of FGF8b treatment (Related to Fig 4).

RC17 cells were patterned towards VM and treated with 50, 100 or 300 ng/ml FGF8b from d9-16. Results from cell qRT-PCR (**A**) and immunostainings (**B**) showed 100 ng/ml to be optimal for induction of MHB markers. Scale bar: 100µm (**C**) When FGF8b was withdrawn from the cells, the cells still maintained a highly increased level of EN1 expression 22 days after withdrawal, while the levels of FOXA2 and LMX1A remained the same as control cells which had not received FGF8.

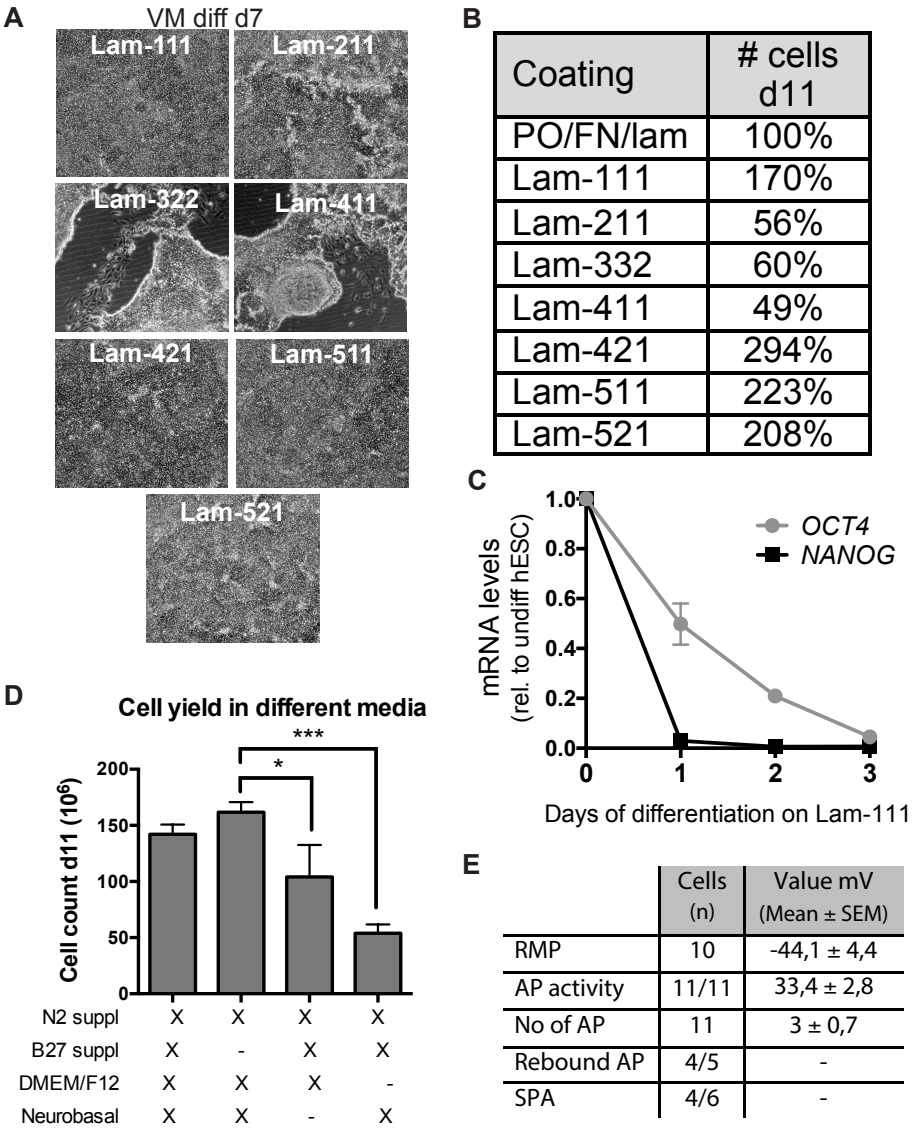

Figure S4. Development of Lam-111-based GMP protocol (related to Figure 5)

(**A)** Neural differentiation of hESCs on different Laminins revealed optimal attachment and yield of neural cells on Lam-111, Lam-421, Lam-511 and Lam-521. (**B)**. Results from cell counts of hESC differentiated on different coatings from d0-11 and counted on d11. Counts are shown relative to a coating of research-grade polyornithine, fibronactin and sarcoma-derived laminin (PO/FN/lam). (**C**) Neural differentiation on Lam-111 matrix was accompanied by a rapid downregulation of pluripotency markers as measured by qRT-PCR. (**D**) Testing of different combinations of basic medium showed highest cell yield in mixed DMEM/F12+Neurobasal medium with N2 supplement, whereas addition of B27 supplement did not increase cell yield. (**E**) Results from patch clamp electrophysiology of GMP-derived neurons *in vitro* (Figure 5G-J). RMP= Resting membrane potential, AP = Action potential, SPA = Spontaneous postsynaptic activity.

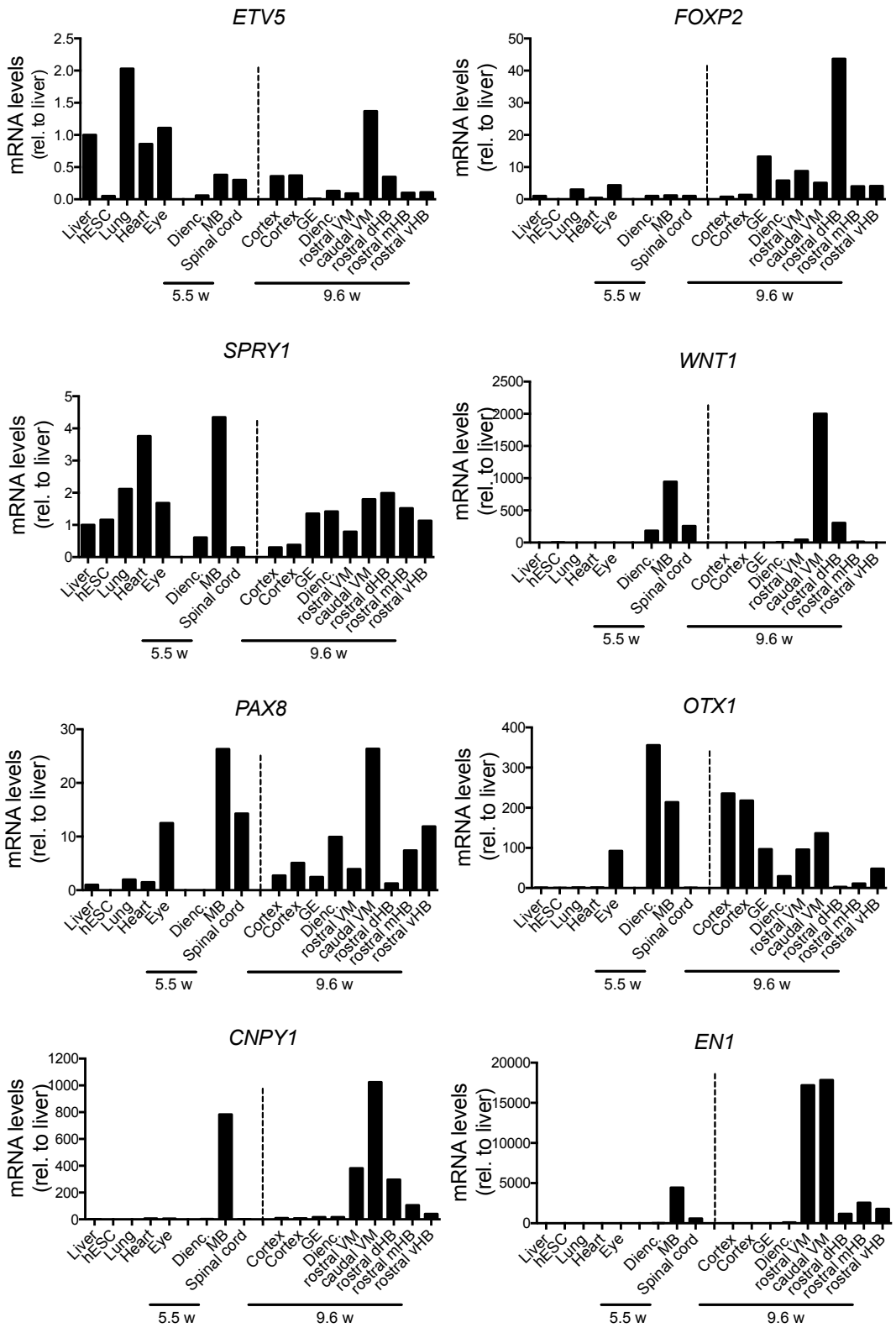

Figure S5. Validation of qRT-PCR primers in sub-dissected human fetal tissue (related to Figure 6)

Primers for qRT-PCR were validated for producing specific signals in sub-dissected human fetal tissue of 2 different ages (5.5 and 9.6 weeks post-conception). Data is shown as FC relative to fetal liver. Dienc: Diencephalon, MB: Whole midbrain, GE: Ganglionic emninence, VM: Ventral midbrain, dHB: Dorsal hindbrain, mHB: Medial hindbrain, vHB: Ventral hindbrain.

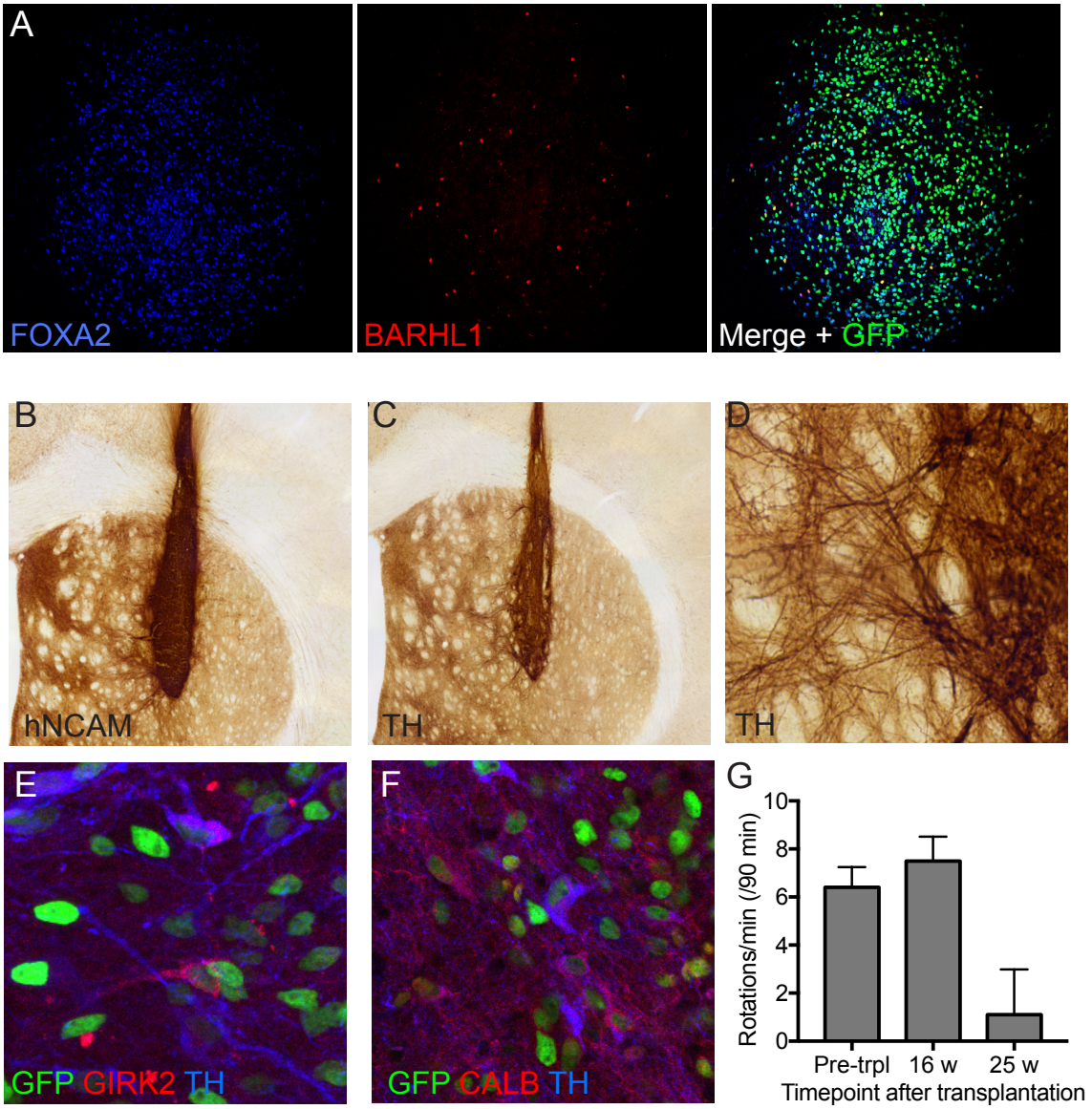

Figure S6. Assessment of BARHL1 in GMP grafts and i*n vivo* validation of GMP protocol with H9 cell line (related to Figure 6)

(**A**) Image of RC17 GMP graft (25 wks) stained for FOXA2, BARHL1 and visualized by graft-specific expression of nuclear GFP. Quantification of BARHL1+ cells out of total graft cells (GFP+) showed that just 1.90%± 0.43%, n = 3 were double-positive (**B-D**) Representative images of hNCAM and TH in 16 week old grafts from H9 cells generated via the GMP protocol showing neuron-rich grafts with extensive host brain innervation (hNCAM overview in **B**), as well as a high TH-density (**C**) with TH+ fibers extending into the host striatum (**D**). (**E, F**) The grafted TH+ neurons co-expressed GIRK2 and CALB (Grafted cells are visualised by expression of nuclear GFP) (**G**) The grafts induced reduction in amphetamine-induced rotations as assessed 25 weeks after transplantation.

Batch #	Graft survival	Animals (n)	Graft site	Rat host strain	Immuno-suppression	# grafted cells	Avg. DA yield (TH+/100.000)	Avg. Volume (mm^3/100,000)	Avg DA density (TH+/mm^3)	Included in DESeq2+PCA	Additional qRT-PCR validation (Fig. 2G+H)	Included in Term diff qRT-PCR (Fig. 1G)	Publication
Batch 1	6 wks	7/7	Str.	SD	Ciclo	$3*10^5$	3711	1,008	3790	DA-high			1
Batch 2	6 wks	8/8	Str.	SD	Ciclo	$3*10^5$	4616	1,141	3972	DA-high			1
Batch 3	6 wks	7/7	Str.	SD	Ciclo	$3*10^5$	8660	2,394	3579	DA-high			1
Batch 4	6 wks	7/7	Str.	SD	Ciclo	$3*10^5$	5597	1,366	4001	DA-high			1
Batch 5	18 wks	7/10	Str.	SD	Ciclo	$3*10^5$	19876	4,413	4479				1
Batch 6	24 wks	6/6	Str.	AT	-	$1.5*10^5$	9260	2,897	3335	DA-high			2
Batch 7	16 wks	13/14	Str.	LH	Ciclo	$3*10^5$	273	0,090	3099	DA-low			
Batch 8	24 wks	4/9	SN	AT	-	$1*10^5$	38	ND	ND		X	X	
Batch 11	21 wks	9/16	Str.	LH	Ciclo	$3*10^5$	266	0,118	2425	DA-low			
Batch 12	24 wks	8/8	SN	AT	-	$1*10^5$	4007	ND	ND				2
Batch 13	A: 6 wks	3/4	Str.	SD	Ciclo	$2*10^5$	212	0,099	2485	DA-low			
	B: 6 wks	3/4	Str.	SD	Ciclo	$2*10^5$	176	0,072	1583				
Batch 14	6 wks	5/6	Str.	SD	Ciclo	$2*10^5$	170	0,049	4080	DA-low			3
Batch 16	6 wks	4/4	Str.	SD	Ciclo	$1.5*10^5$	1052	1,606	658			X	
Batch 17	24 wks	10/10	Str.	AT	-	$3*10^5$	2198	0,537	7387		X		3
Batch 18	A: 4 wks	4/4	Str.	SD	Ciclo	$3*10^5$	581	0,085	5936		X	X	
	B: 16 wks	5/8	Str.	SD	Ciclo	$3*10^5$	1011	0,231	5894				
Batch 19	A: 4 wks	3/4	Str.	SD	Ciclo	$3*10^5$	36	0,028	923		X	X	
	B: 16 wks	7/8	Str.	SD	Ciclo	$3*10^5$	261	0,057	4772				
Batch 20	6 wks	4/4	Str.	SD	Ciclo	$1.5*10^5$	755	0,294	3791			X	
Batch 21	6 wks	4/4	Str.	SD	Ciclo	$1.5*10^5$	13	0,026	527			X	
Batch 22	A: 18 wks	4/4	Str.	SD	Ciclo	$2*10^5$	6868	1,380	3573		X	X	3
	B: 24 wks	6/6	Str.	AT	-	$3*10^5$	5822	1,820	3536			X	3
Batch 23	A: 18 wks	3/4	Str.	SD	Ciclo	$2*10^5$	4141	1,308	4754	DA-high		X	3
	B: 24 wks	6/6	Str.	AT	-	$3*10^5$	3549	0,881	3999	DA-high			3
Batch 24	6 wks	2/2	Str.	SD	Ciclo	$4*10^5$	9	0,043	345	DA-low		X	
Batch 25	18 wks	4/4	Str.	SD	Ciclo	$4*10^5$	7.5	0.016	580	DA-low		X	
Batch 26	16 wks	5/7	Str.	SD	Ciclo	$2.4*10^5$	963	0,856	1729			X	
Batch 27	16 wks	5/8	Str.	SD	Ciclo	$3*10^5$	3970	0,828	4461	DA-high		X	
Batch 28	16 wks	3/7	Str.	SD	Ciclo	$3*10^5$	1117	0,208	4869			X	
Batch 29	18 wks	5/5	Str.	SD	Ciclo	$1.5*10^5$	7054	1,640	4509		X	X	
Batch 30	18 wks	4/4	SN	SD	Ciclo	$0.75*10^5$	4484	1,532	2911		X	X	
Batch 31	20 wks	9/9	Str.	LH	Ciclo	$3.4*10^5$	5200	1,430	3787			X	

Table S1. Overview of graft experiments used for marker correlations (related to Figures 1 and 2)

Table shows details on each grafting experiment. All grafts were performed with H9 cells using the research-grade protocol (Kirkeby et al 2012). Animals (n) are shown as number of animals with surviving grafts out of total number of grafted animals. Only animals with surviving grafts were included in the quantitative analyses. Graft site: Str. = striatum, SN = substantia nigra. Rat host strain: SD = Sprague-Dawley, LH = Lister-hooded, AT = Athymic Crl:NIH-Foxn1rnu, Immunosuppresion: Ciclo = Daily intraperitoneal injections of Ciclosporin (10 mg/kg), starting the day before transplantation. Publications = Published studies in which these experiments have been included. 1: Kirkeby et al., 2012, 2: Grealish et al., 2014, 3: Grealish et al., 2015.

Table S2 (separate xlsx sheet). Results from DESeq2 analysis (related to Figure 2)

The table shows log2 fold change of gene expression in the DA-high group versus the DA-low group together with the p-value and adjusted p-values (padj) for each gene.

Gene	Expression domain	Reference
ANGPTL4	Hypothalamus	Kim et al., 2010
CNPY1	MHB	Hirate and Okamoto, 2006
EN1/2	MHB/caudal VM	Kee et al 2016; Veenvliet et al., 2013; Ye et al., 2001; Zhong et al., 2010
EPHA3	Thalamus/STN	Kee et al 2016; Kudo et al., 2005
ETV4/5	MHB	Lahti et al., 2012; Raible and Brand, 2001
FEZF1	Hypothalamus	Kurrasch et al., 2007
LEFTY1/2	Diencephalon	Bisgrove et al., 1999; Long et al., 2003
NPW	Hypothalamus/pituitary	Dun et al., 2003
PAX5	MHB	Asano and Gruss, 1992
PAX8	MHB	Pfeffer et al., 1998
PTHLH	Pituitary	Campos et al., 1991
SP5	MHB	Tallafuss et al., 2001
TGFB1	Diencephalon+dorsal MB	Mecha et al., 2008
TLE4	MHB	Heimbucher et al., 2007
WNT1/4	MHB	Hollyday et al., 1995
WNT7B	Diencephalon	Garda et al., 2002; Hollyday et al., 1995

Table S3. Supplemental references for diencephalic and MHB genes (related to Figure 2)

The table shows selected references describing the expression domains of genes shown to be differentially expressed in our DA-low versus DA-high cell batches.

Reagent name	Supplier	Cat number
For Differentiation		
StemMACS iPS Brew	Miltenyi	130-104-368
Lam-521	BioLamina	LN-521
Lam-111	BioLamina	LN-111
DPBS +Ca +Mg (CTS)	LT	A12858-01
EDTA	LT	15575-020
PBS -/- CTS	LT	A12856-01
DMEM:F12	LT	21331-020
Neurobasal CTS	LT	A13712-01
N2 supplement CTS	LT	A13707-01
B27 supplement w/o vitamin A	LT	12587-010
L Glutamine	LT	25030-081
AccutaseGMP	Innov. Cell Tech	AccutaseGMP
SB431542	Miltenyi	130-105-336
CHIR99021 (10 mM in DMSO solution)	Miltenyi	130-106-539
Y-27632 dihydrochloride	Miltenyi	130-103-922
Noggin GMP	R&D	6057-GMP
BDNF GMP	R&D	248-GMP
SHH C24II Premium Grade	Miltenyi	130-095-727
L-Ascorbic Acid	Sigma	A4403-100MG
FGF8b Premium Grade	Miltenyi	130-095-740
For Transplantation		
HBSS (no Ca/Mg, no Phenol Red)	LT	14175053
Pulmozyme (Dornase Alpha)	Roche	11899

Table S4. List of GMP reagents used for cell culture ad differentiation (related to Figure 5)

Supplemental Experimental procedures

Surgical procedures

All rats received a 6-OHDA lesion of the MFB as described in (Kirik et al., 1998). Briefly, rats were anesthetized with isoflourane (2–4% with carrier gases oxygen and nitrous oxide) or intraperitonal injection of Fentanyl and Medetomidine (20:1), and put in a stereotaxic frame. The MFB was targeted with an injection of 3-4 µl 0.01-0.02% L-ascorbic acid saline solution containing a total amount of 12-14 µg of 6-OHDA (freebase). The stereotaxic coordinates for lesioning were adjusted to the age and weight of the animals. For intrastriatal transplantation of hESCs, cell suspensions of 50,000 - 100,000 cells/µl were transplanted in 1-2 deposits of 2 µl each at the following coordinates: (1) AP: +1.2, ML: -2.6; (2) AP: +0.5, ML: -3.0; and DV -3.7 to -4.5 from dura, with the tooth bar set to -2.4. The cells were injected at a rate of 0.5 µl per minute, and the capillary was left in place for a further 3 min before being retracted. See Table S1 for total cell number grafted in each experiment. For intranigral transplantations, cell suspensions of 37,500 - 50,000 cells/µl were transplanted in 1 deposit of 2 µl at the following coordinates: AP: -4.6, ML: -2.2 and DV -7 from dura, with the tooth bar set to -2.4

Behavioural analysis

Rotational asymmetry was assessed in automated rotometer bowls which were modelled after the design of Ungerstedt and Arbuthnott (1970). Amphetamine-induced rotation was induced by intraperitoneal injection of 2.5 mg/kg *d*-amphetamine hydrochloride (Sigma Chemicals, UK) dissolved in sterile saline and behaviour was recorded over a period of 90 min. All rotation scores were expressed as an average of ipsilateral rotations minus contralateral rotations (Kirkeby et al, 2012). Spontaneous paw-use asymmetry was assessed as explorative behaviour in a glass cylinder. The behaviour was video recorded over a period of 5 minutes and scored post hoc. Paw use preference was expressed as contralateral cylinder touches as percent of total (Left/(Left+Right) x 100%).

Immunohistochemistry

At ended experiments, rats were terminally anaesthetized with sodium pentobarbital and sacrificed by transcardial perfusion with a 4% paraformaldehyde solution (pH = 7.4). Brains were post-fixed for an additional 2 hours before cryopreservation in a 25-30% sucrose solution. Tissue was sectioned coronally for immunohistochemistry on a freezing sledge microtome at 35-40µm thickness in series of 1:8 or 1:12. All washing steps were done in 0.1 M phosphate buffered saline with potassium (KPBS) and all incubations were done in 3-5 % serum (secondary antibody host species) + 0.25 % Triton X-100 in KPBS. Sections were incubated with primary antibody over night at room temperature (RT) or over 60 hours at 4°C (see list of antibodies and dilutions below). For immunofluorescence, tissue was incubated with fluorophore-conjugated secondary antibodies (DAKO) for 1-3 hours at RT. Confocal fluorescent images were captured using a Leica DMRE confocal microscope equipped with green helium/neon, standard helium/neon and argon lasers. For DAB stainings, tissue was incubated with secondary biotinylated-horse antibodies (1:200, Vector Laboratories) for 1-3 hours at RT, followed by an amplification step with streptavidin–biotin for 1-2 hours at RT. Detection of primary-secondary antibody complexes was performed using peroxidase driven precipitation of di-amino-benzidine (DAB). In this step, sections were incubated in 0.05 % DAB for 1.5 minutes before addition of 0.01% H2O2 for 1.5 minutes. The sections were finally mounted on gelatin coated slides, dehydrated in an ascending series of alcohols, cleared in xylene and coverslipped with DPX mountant.

Quantification of graft volumes

To estimate the graft volumes, the sections were scanned using a DUOSCAN f40 AGFA and analysed with Image J software (NIH, v1.49). The graft area was extrapolated in every section of 1:8 or 1:12 series that showed HuNu+ staining, and the volume of the grafts were calculated using Cavalieri's principle (Cavalieri, 1966). For those animals where HuNu stained sections were not available, hNCAM was used for volume estimations. Since hNCAM labels not only nuclei but also processes, only the densest core of the grafts was included in the measurements. The graft volume was normalized to 100,000 transplanted cells in order enable comparison between experiments.

Human fetal tissue

Human fetal tissue was obtained in accordance with existing guidelines from legally terminated embryos under informed consent from women seeking elective abortions and with approval of the Swedish National Board of Health and Welfare. The gestational age of each embryo was determined by measuring the crown-to-rump length, and embryos

were staged according to weeks post-conception. For immunohistochemistry, the brain was isolated from each embryo and the diencephalic and ventral midbrain regions were subdissected and fixed in 4% paraformaldehyde overnight. Subsequently, the tissue was cryoprotected in 30% sucrose before embedding in O.C.T Tissue-Tek (Sakura FineTek, Europe BF) for cryo-sectioning and staining.

Cell culture and GMP differentiation protocol

Reagents used for VM differentiation according to GMP protocol can be found in Table S4. Undifferentiated RC17 cells were maintained on Lam-521 (0.5 µg/cm2) coated plates in iPS Brew and passaged weekly with EDTA (0.5 mM). To start differentiations (day 0), hESC colonies were detached from the culture dish with EDTA (0.5 mM) to yield a cell suspension of small colonies (2-5 cells in each). Cell concentration in the resulting colony suspension was quantified by taking out an aliquot of colonies for dissociation into single cells by accutase treatment for subsequent cell counting. Differentiation was initiated by plating of colonies onto Lam-111 (10 µg/cm2) coated cell cultures plates in differentiation medium at a density of 10,000 cells/cm2. Differentiation medium from day 0-9 consisted of DMEM/F12:Neurobasal (1:1), N2 supplement (1:100), SB431542 (10 µM), rhNoggin (100 ng/ml), SHH-C24II (200 ng/ml) and CHIR99021 (0.7 µM). On d11 of differentiation, cells were dissociated to single cells with accutase and replated onto lam-111 coated plates at a density of 800,000 cells/cm2 in Neurobasal, B27 supplement without vitamin A (1:50), brain-derived neurotrophic factor (BDNF) (20 ng/ml) and ascorbic acid (200 mM). FGF8b (100 ng/ml) could be added to the cells at different timepoints. Rock inhibitor (Y-27632, 10 µM) was added to the cells at replating steps (day 0 and 11). For terminal maturation of the cell in vitro, db-cAMP (0.5 mM) and DAPT (1 µM) was added to the medium from day 16 and onwards. For immunofluorescent staining of in vitro experiments, cells were fixed in 4% PFA and incubated overnight with relevant primary antibodies (see list of antibodies below) before addition of secondary fluorophore-conjugated antibodies (DAKO).

Quantitative reverse-transcription PCR (qRT-PCR)

RNA was isolated from cell cultures using the RNeasy Micro kit and from human tissue using the RNeasy lipid tissue kit (QIAGEN). Reverse transcription was performed with random hexamer primers and Superscript III enzyme (Invitrogen), using up to 1 µg of RNA from each sample. The cDNA was pipetted together with Sybr green mastermix (Roche) using the Bravo instrument (Agilent) and analyzed by quantitative PCR on a LightCycler 480 instrument using a 2-step protocol with a 60oC annealing/elongation step. All quantitative RT-PCR (qRT-PCR) samples were run in technical triplicates, and the average Ct-values were used for calculations. Data are represented using the DDCt method. All fold changes are calculated as the average fold change based on 2 different housekeeping genes (b-actin and GAPDH). See Table S6 for a complete list of primers used in this study.

Electrophysiology

Patch-clamp electrophysiology was performed on RC17 hESCs differentiated to a VM fate at day 45 post-differentiation. Cells grown on coverslips were submerged in a continuously flowing Krebs solution (119 mM NaCl, 2.5 mM KCl, 1.3 mM MgSO4, 2.5 mM CaCl2, 25 mM Glucose and 26 mM NaHCO3) gassed with 95% O2 - 5% CO2 at 28°C. Recordings were made with a Multiclamp 700B amplifier (Molecular Devices), using borosilicate glass pipettes (3–7 MOhm) filled with 122.5 mM potassium gluconate, 12.5 mM KCl, 0.2 mM EGTA, 10 mM Hepes, 2 mM MgATP, 0.3 mM Na3GTP and 8 mM NaCl adjusted to pH 7.3 with KOH. Data were acquired with pClamp 10.2 (Molecular Devices); current was filtered at 0.1 kHz and digitized at 2kHz. Cells with neuronal morphology with round cell body were selected for whole-cell patch clamp. Resting membrane potentials were monitored immediately after breaking-in in current-clamp mode. Thereafter, cells were kept at a membrane potential of -60mV to -80mV, and 500ms currents were injected from -20pA to +90pA with 10pA increments to induce action potentials. For rebound depolarizations the cells were injected with a train of small currents of 20 pA to induce action potentials. Spontaneous post-synaptic currents were recorded at -60 mV using the same internal solution.

Flow cytomery

For labelling of FOXA2, cells were fixed using the FOXP3 staining buffer set (Miltenyi), and labelled with antibodies for 30 min at 4C prior washing and analysis. Antibodies were kindly provided by Miltenyi Biotec as a gift. For CORIN labelling, cells were stained live for 20 min on ice. Cells were analysed on a FACSAria III instrument and subjected to compensation based on single-stained controls.

List of primer sequences used in this study

Gene	Full gene name	Primer sequence (fwd/rev)
AADC	DDC (DOPA decarboxylase)	GGGGACCACAACATGCTGCTCC
		AATGCACTGCCTGCGTAGGCTG
ACTB	beta-actin	CCTTGCACATGCCGGAG
		GCACAGAGCCTCGCCTT
BARHL1	BarH-like homeobox 1	GTACCAGAACCGCAGGACTAAA
		AGAAATAAGGCGACGGGAACAT
BARHL2	BarH-like homeobox 2	GGAGATTACGAGTAGCCGTGAG
		AAGCTACGCTCCAGTTGATTGA
CORIN	corin, serine peptidase	CATATCTCCATCGCCTCAGTTG
		GGCAGGAGTCCATGACTGT
CNPY1	Canopy FGF signaling regulator1	TTGGCCTCTCAAACACCATTCT
		GAGCGAAACAAAACGCAATCAC
EN1	Engrailed 1	CGTGGCTTACTCCCCATTTA
		TCTCGCTGTCTCTCCCTCTC
ETV5	Ets Variant 5	TCATCCTACATGAGAGGGGGTT
		GACTTTGCCTTCCAGTCTCTCA
FOXA2	forkhead box A2	CCGTTCTCCATCAACAACCT
		GGGGTAGTGCATCACCTGTT
FOXG1	forkhead box G1 (BF1)	TGGCCCATGTCGCCCTTCCT
		GCCGACGTGGTGCCGTTGTA
FOXP2	Forkhead box P2	ATGAGCACTCTAAGCAGCCAAT
		GTTGCAGATGCAGCAGTTCTAC
GAPDH	Glyceraldehyde-3-phosphate dehydrogenase	TTGAGGTCAATGAAGGGGTC
		GAAGGTGAAGGTCGGAGTCA
HOXA2	Homeobox A2	CGTCGCTCGCTGAGTGCCTG
		TGTCGAGTGTGAAAGCGTCGAGG
LHX2	LIM homeobox 2	GGGCGACCACTTCGGCATGAA
		CGTCGGCATGGTTGAAGTGTGC
LMX1A	LIM homeobox transcription factor a	CGCATCGTTTCTTCTCCTCT
		CAGACAGACTTGGGGCTCAC
LMX1B	LIM homeobox transcription factor b	CTTAACCAGCCTCAGCGACT
		TCAGGAGGCGAAGTAGGAAC
NANOG	Nanog homeobox	TTGGGACTGGTGGAAGAATC
		GATTTGTGGGCCTGAAGAAA
NKX2.1	NK2 homeobox 1	AGGGCGGGGCACAGATTGGA
		GCTGGCAGAGTGTGCCCAGA
NURR1	NR4a2	CAGGCGTTTTCGAGGAAAT
		GAGACGCGGAGAACTCCTAA
OCT4	POU5F1	TCTCCAGGTTGCCTCTCACT
		GTGGAGGAAGCTGACAACAA
OTX1	Orthodenticle homeobox 1	TATAAGGACCAAGCCTCATGGC
		TTCTCCTCTTTCATTCCTGGGC
OTX2	Orthodenticle homeobox 2	ACAAGTGGCCAATTCACTCC
		GAGGTGGACAAGGGATCTGA
PAX6	Paired box 6	TGGTATTCTCTCCCCTCCT
		TAAGGATGTTGAACGGGCAG
PAX8	Paired box 8	ATAGCTGCCGACTAAGCATTGA
		ATCCGTGCGAAGGTGCTTT
SHH	Sonic hedgehog	CCAATTACAACCCCGACATC
		AGTTTCACTCCTGGCCACTG
SIX3	SIX homeobox 3	ACCGGCCTCACTCCCACACA
		CGCTCGGTCCAATGGCCTGG
SIX6	SIX homeobox 6	CTCAACAAGAATGAGTCGGTGC
		ACTCCTTGGTGAACTTGTGGTT
SPRY1	Sprouty 1	GCCCTGGATAAGGAACAGCTAC
		GCCGAAATGCCTAATGCAAAGA
TH	Tyrosine hydroxylase	CGGGCTTCTCGGACCAGGTGTA
		CTCCTCGGCGGTGTACTCCACA
WNT1	Wingless-type MMTV integration site family, member 1	GAGCCACGAGTTTGGATGTT
		TGCAGGGAGAAAGGAGAGAA

List of antibodies used in this study

Antigen	Species	Company (cat.no.)	Dilution
BARHL1	Rabbit	Novus Biologicus (NBP1-86513)	1:1000
CALB	Rabbit	Swant (CB38)	1:1000
CORIN	Rat	R&D Systems (MAB2209)	1:500 (FC)
EN1	Mouse	DSHB (4G11)	1:20
FOXA2	Goat	Santa Cruz (M-20)	1:500
FOXA2-PE	Mouse	Miltenyi Biotec (130-107-826)	1:10 (FC)
GIRK2	Goat	Millipore (AB65096)	1:200
HuNu	Mouse	Chemicon (MAB1281)	1:200
LMX1A/B	Rabbit	Millipore (AB10533)	1:1000
hNCAM	Mouse	Santa Cruz (SC106)	1:100
NKX2.1	Rabbit	Abcam (ab133737)	1:500
PITX2	Sheep	R&D systems (AF7388)	1:2000
TH	Mouse	Chemicon (MAB318)	1:2000
TH	Rabbit	Abcam (AB152)	1:1000

FC: antibodies used for flow cytometry

Supplemental References

Asano, M., and Gruss, P. (1992). Pax-5 is expressed at the midbrain-hindbrain boundary during mouse development. Mech Dev *39*, 29-39.

Bisgrove, B.W., Essner, J.J., and Yost, H.J. (1999). Regulation of midline development by antagonism of lefty and nodal signaling. Development *126*, 3253-3262.

Campos, R.V., Asa, S.L., and Drucker, D.J. (1991). Immunocytochemical localization of parathyroid hormone-like peptide in the rat fetus. Cancer Res *51*, 6351-6357.

Cavalieri B (1966) Geometria degli indivisibli. Unione Tipigrafico, Editrice, New York

Dun, S.L., Brailoiu, G.C., Yang, J., Chang, J.K., and Dun, N.J. (2003). Neuropeptide W-immunoreactivity in the hypothalamus and pituitary of the rat. Neurosci Lett *349*, 71-74.

Garda, A.L., Puelles, L., Rubenstein, J.L., and Medina, L. (2002). Expression patterns of Wnt8b and Wnt7b in the chicken embryonic brain suggest a correlation with forebrain patterning centers and morphogenesis. Neuroscience *113*, 689-698.

Grealish, S., Diguet, E., Kirkeby, A., Mattsson, B., Heuer, A., Bramoulle, Y., Van Camp, N., Perrier, A.L., Hantraye, P., Bjorklund, A*., et al.* (2014). Human ESC-derived dopamine neurons show similar preclinical efficacy and potency to fetal neurons when grafted in a rat model of Parkinson's disease. Cell Stem Cell *15*, 653-665.

Grealish, S., Heuer, A., Cardoso, T., Kirkeby, A., Jonsson, M., Johansson, J., Bjorklund, A., Jakobsson, J., and Parmar, M. (2015). Monosynaptic Tracing using Modified Rabies Virus Reveals Early and Extensive Circuit Integration of Human Embryonic Stem Cell-Derived Neurons. Stem Cell Reports *4*, 975-983.

Heimbucher, T., Murko, C., Bajoghli, B., Aghaallaei, N., Huber, A., Stebegg, R., Eberhard, D., Fink, M., Simeone, A., and Czerny, T. (2007). Gbx2 and Otx2 interact with the WD40 domain of Groucho/Tle corepressors. Mol Cell Biol *27*, 340-351.

Hirate, Y., and Okamoto, H. (2006). Canopy1, a novel regulator of FGF signaling around the midbrain-hindbrain boundary in zebrafish. Curr Biol *16*, 421-427.

Hollyday, M., McMahon, J.A., and McMahon, A.P. (1995). Wnt expression patterns in chick embryo nervous system. Mech Dev *52*, 9-25.

Kim, H.K., Youn, B.S., Shin, M.S., Namkoong, C., Park, K.H., Baik, J.H., Kim, J.B., Park, J.Y., Lee, K.U., Kim, Y.B*., et al.* (2010). Hypothalamic Angptl4/Fiaf is a novel regulator of food intake and body weight. Diabetes *59*, 2772-2780.

Kirik, D., Rosenblad, C., and Bjorklund, A. (1998). Characterization of behavioral and neurodegenerative changes following partial lesions of the nigrostriatal dopamine system induced by intrastriatal 6-hydroxydopamine in the rat. Exp Neurol *152*, 259-277.

Kirkeby, A., Grealish, S., Wolf, D.A., Nelander, J., Wood, J., Lundblad, M., Lindvall, O., and Parmar, M. (2012). Generation of regionally specified neural progenitors and functional neurons from human embryonic stem cells under defined conditions. Cell Rep *1*, 703-714.

Kudo, C., Ajioka, I., Hirata, Y., and Nakajima, K. (2005). Expression profiles of EphA3 at both the RNA and protein level in the developing mammalian forebrain. J Comp Neurol *487*, 255-269.

Kurrasch, D.M., Cheung, C.C., Lee, F.Y., Tran, P.V., Hata, K., and Ingraham, H.A. (2007). The neonatal ventromedial hypothalamus transcriptome reveals novel markers with spatially distinct patterning. J Neurosci *27*, 13624-13634.

Lahti, L., Peltopuro, P., Piepponen, T.P., and Partanen, J. (2012). Cell-autonomous FGF signaling regulates anteroposterior patterning and neuronal differentiation in the mesodiencephalic dopaminergic progenitor domain. Development *139*, 894-905.

Long, S., Ahmad, N., and Rebagliati, M. (2003). The zebrafish nodal-related gene southpaw is required for visceral and diencephalic left-right asymmetry. Development *130*, 2303-2316.

Mecha, M., Rabadan, M.A., Pena-Melian, A., Valencia, M., Mondejar, T., and Blanco, M.J. (2008). Expression of TGF-betas in the embryonic nervous system: analysis of interbalance between isoforms. Dev Dyn *237*, 1709-1717.

Pfeffer, P.L., Gerster, T., Lun, K., Brand, M., and Busslinger, M. (1998). Characterization of three novel members of the zebrafish Pax2/5/8 family: dependency of Pax5 and Pax8 expression on the Pax2.1 (noi) function. Development *125*, 3063-3074.

Raible, F., and Brand, M. (2001). Tight transcriptional control of the ETS domain factors Erm and Pea3 by Fgf signaling during early zebrafish development. Mech Dev *107*, 105-117.

Tallafuss, A., Wilm, T.P., Crozatier, M., Pfeffer, P., Wassef, M., and Bally-Cuif, L. (2001). The zebrafish buttonhead-like factor Bts1 is an early regulator of pax2.1 expression during mid-hindbrain development. Development *128*, 4021-4034.

Ungerstedt, U., and Arbuthnott, G.W. (1970). Quantitative recording of rotational behavior in rats after 6-hydroxy-dopamine lesions of the nigrostriatal dopamine system. Brain Res *24*, 485-493.

Veenvliet, J.V., Dos Santos, M.T., Kouwenhoven, W.M., von Oerthel, L., Lim, J.L., van der Linden, A.J., Koerkamp, M.J., Holstege, F.C., and Smidt, M.P. (2013). Specification of dopaminergic subsets involves interplay of En1 and Pitx3. Development *140*, 3373-3384.

Ye, W., Bouchard, M., Stone, D., Liu, X., Vella, F., Lee, J., Nakamura, H., Ang, S.L., Busslinger, M., and Rosenthal, A. (2001). Distinct regulators control the expression of the mid-hindbrain organizer signal FGF8. Nat Neurosci *4*, 1175-1181.

Zhong, S.C., Chen, X.S., Cai, Q.Y., Luo, X., Chen, X.H., Liu, J., and Yao, Z.X. (2010). Dynamic expression and heterogeneous intracellular location of En-1 during late mouse embryonic development. Cells Tissues Organs *191*, 289-300.